

MICROSTRUCTURE AND HARDNESS PROFILES OF AHSS SUBJECTED TO SIMULATED LASER WELDING THERMAL CYCLES

MORAWIEC Mateusz ^a, STANO Sebastian ^b, RÓŻAŃSKI Maciej ^b

^a *Institute of Engineering Materials and Biomaterials, Silesian University of Technology, Gliwice, Poland, EU, mateusz.morawiec@polsl.pl*

^b *Institute of Welding, Gliwice, Poland, EU, sebastian.stano@is.gliwice.pl, maciej.rozanski@is.gliwice.pl*

Abstract

This work presents the comparative results of twin-spot laser welding of complex phase and transformation induced plasticity steels. Both steels include Nb and Ti microalloyed elements. Tests of dual beam laser welding were carried out using keyhole welding. The sheets were welded with two different power beam distributions in order to determine the effect of simulated thermal cycles on microstructure and hardness profiles. The power distributions between the beams were 50:50 and 70:30 %. The microstructural constituents in the fusion zone, heat affected zone and base metal were identified using light microscopy and scanning electron microscopy. It was found that the change of beam distribution affects morphological details of the martensite and hardness.

Keywords: AHSS, twin-spot laser welding, dual beam, microalloying

1. INTRODUCTION

One of the main problems in case of laser welding of high strength steels is softening phenomenon that occurs in welds [1, 2]. The group of high strength steels includes the AHSS (Advanced High Strength Steel), which are multiphase steels containing martensite, bainite, ferrite and retained austenite in their microstructure [3-7]. The AHSS are manufactured using relatively complicated heat treatments allowing creation of multiphase microstructures [8-11]. Grajcar et al. [8] investigated the influence of laser welding of Transformation Induced Plasticity steels on their microstructure and hardness. They suggested that using twin-spot laser welding may reduce the hardness of welded material. Because of Nb and Ti micro-additions in chemical composition of analyzed steels, the precipitation kinetics in welding processes needs to be taken into consideration [12-15]. Recently, Grajcar et al. [8] analyzed the effect of laser welding on the microstructure and hardness profiles of Nb-microalloyed TRIP steel.

Because AHSS exhibit high hardness of laser welds, the dual beam laser welding can be used. Double beam welding should decrease the dynamics of thermal cycles, reducing the cooling rate of welded material. The reduction of cooling rate can be attained because of the addition of thermal energy to the material by a second beam. The twin-spot laser welding allows us to re-melt the welded material, eventually to use the second beam for heat treatment after welding. The decrease in a cooling rate increases the time of thermal exposition on a microstructure of welded material. Thus, there is time for diffusional processes which may occur leading to beneficial decrease in hardness of welds.

2. EXPERIMENTAL PROCEDURE

To determine the effect of different thermal cycles on microstructure and hardness, two steels were joined using twin-spot laser welding. The first one was industrially hot-rolled and controlled cooled CPW800 steel. The sheet of dimensions 150 x 300 mm and 2.5 mm in thickness was prepared for laser welding. The second material was thermomechanically rolled TRIP steel with controlled cooling directly from final rolling temperature. To ensure the stabilization of retained austenite the steel was isothermally held at 350 °C for 600

s. In this steel the Si content was decreased because of its negative influence on hot-dip galvanizing. Instead the steel contains increased Al addition, which prevents precipitation of carbides (similarly to silicon). The sheet of 100 mm width and 2 mm in thickness was prepared. Both steels include Nb and Ti micro-additions in their chemical composition. Microalloying elements were added to prevent grain growth by the formation of dispersive carbonitrides. The chemical composition and carbon equivalent calculated based on the equation (1) for both steels are shown in **Table 1**.

$$C_{eq} = C + \frac{Mn}{6} + \frac{Si}{24} + \frac{Ni}{40} + \frac{Cr}{5} + \frac{Mo}{4} \% \quad (1)$$

Table 1 Chemical composition of CP and TRIP steels (wt. %)

	C	Mn	Si	Cr	S	P	Nb	Ti	N	Al	Mo	C _{eq}
CP	0.08	1.72	0.56	0.34	0.003	0.010	0.005	0.125	0.002	0.29	0.016	0.46
TRIP	0.24	1.55	0.87	-	0.004	0.010	0.034	0.023	0.0028	0.40	-	0.54

The second beam is created using special optical lens by putting them into a beam path. These optical lens allow us to change the distance and the power distribution between both beams. The distance is changed by manipulating the angle of lens, while the power distribution is changed by changing the position of lens in a beam path. In both steels the beams were set in a tandem mode and the distance between beams was set to 4 mm. **Table 2** shows parameters of laser welding for both steels.

Table 2 Welding parameters

Sample	CP		TRIP	
	1	2	3	4
Maximum beam power, kW	6	6	4	4
Power distribution, %	50:50	70:30	50:50	70:30
Welding speed, m / s	5.5	5.5	4	4
Linear energy, kJ / mm	0.065	0.065	0.060	0.060

3. RESULTS

The microstructure of base metal in case of CP steel is composed of fine-grained ferritic-bainitic matrix with martensitic-austenitic islands of various size (**Figure 1a**). In case of TRIP steel, its microstructure is composed of fine-grained ferritic matrix including bainitic-austenitic islands, martensite and some fraction of retained austenite (**Figure 1b**).

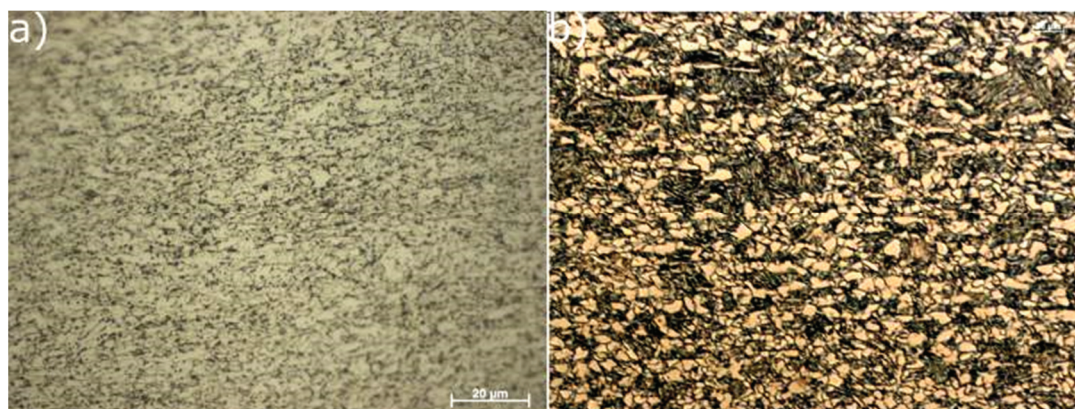


Figure 1 Microstructure of base metal in case of: a) CP steel, b) TRIP steel

The SEM microstructures of fusion zones for CP and TRIP steels welded with different parameters are presented in **Figure 2**. **Figures 2a** and **2b** show the microstructures of CP steel welded with 50:50 and 70:30 % power distribution, while **Figures 2c** and **2d** present in similar way the microstructure of the fusion zone of TRIP steel.

The microstructure of fusion zone for both steels presented in **Figure 2** is composed of lath martensite, martensitic-austenitic (MA) islands and small fraction of retained austenite (RA). Comparing the microstructures presented in **Figures 2a** and **2c** it can be seen that the TRIP steel has more developed morphology of fusion zone compared to the CP steel. The reason for that can be higher carbon equivalent of TRIP steel that increases the vulnerability for martensite creation. The martensite morphology must be also taken into account, which shows defragmentation of the martensite. The defragmentation of martensite is characteristic for tempered martensite, so it can be possible that the presence of second beam leads to tempering-like processes after welding. In case of higher power difference (**Figures 2b** and **2d**) the diffusion-like controlled defragmentation of martensite can proceed. The retained austenite in CP steel is present in form of small grains randomly distributed in the microstructure. In case of TRIP steel the retained austenite can be identified in form of thin films between martensite laths.

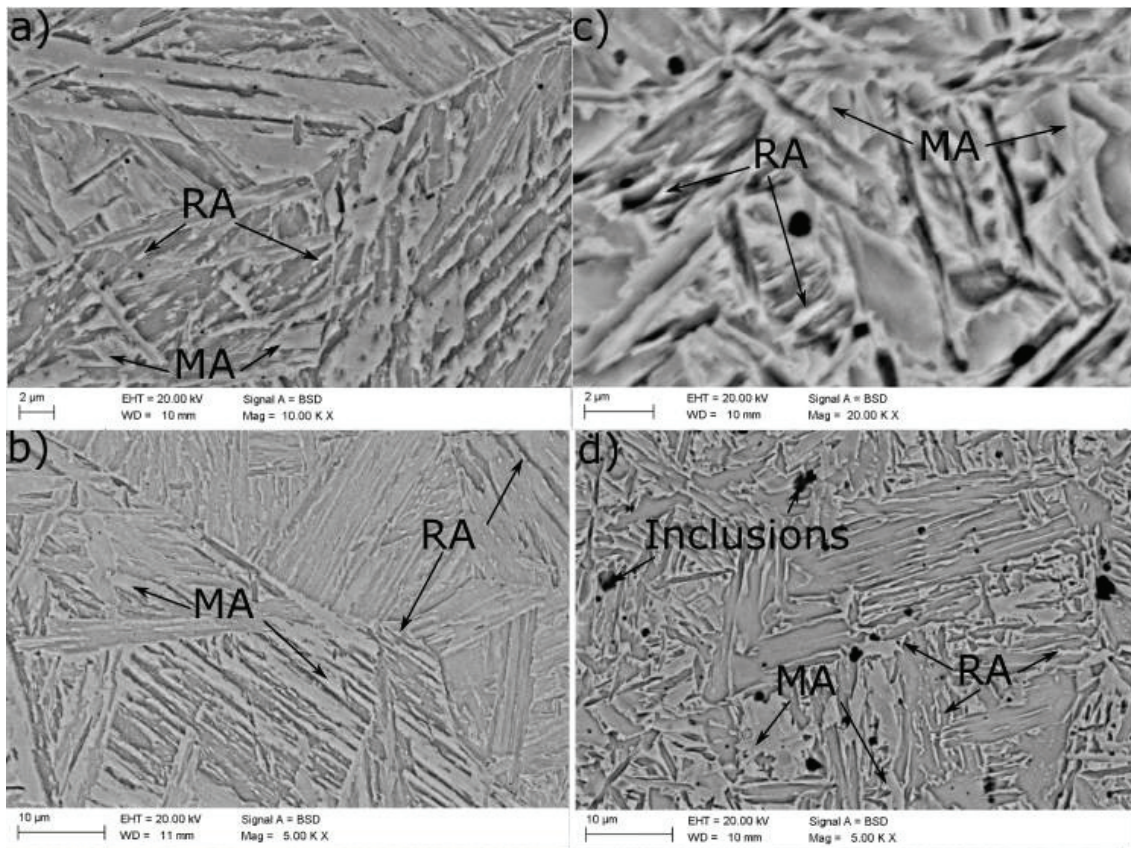


Figure 2 SEM microstructures of fusion zone for different power distribution: (a, b) CP steel with 50:50 and 70:30 % power distribution, (c, d) TRIP steel with 50:50 and 70:30 % power distribution

Figure 3 presents the microstructures of heat affected zones (HAZ) of CP and TRIP steels subjected to different thermal cycles of welding. **Figures 3a** and **3b** show the microstructure of HAZ of CP steel welded with 50:50 and 70:30 % power distributions. **Figures 3c** and **3d** present microstructures of HAZ of TRIP steel welded with analogical parameters. The microstructure of both steels is composed of fine-grained mixture of martensite, bainite, and some fraction of retained austenite. The main difference between CP and TRIP steel is the morphology of the microstructure. The morphology of CP steel is more blocky, when in case of TRIP

steel the morphology is mostly lath-like. It can be seen that the change of power distribution doesn't influence the microstructure of both steels significantly. In both steels the retained austenite was identified in the microstructure of the heat affected zone. In CP steel it can be found on edges of blocky martensite in form of martensitic-austenitic (MA) constituents and in form of small blocky grains. In case of TRIP steel it takes a form of films located between bainite and martensite laths and MA constituents.

The morphology of martensite in the heat affected zone is defragmented similarly to that observed in the fusion zone. This behaviour can be explained by the presence of second beam that decreases the dynamic cycle of laser welding. This phenomenon may lead to a beneficial decrease of the hardness of welds when compared to conventional laser welding.

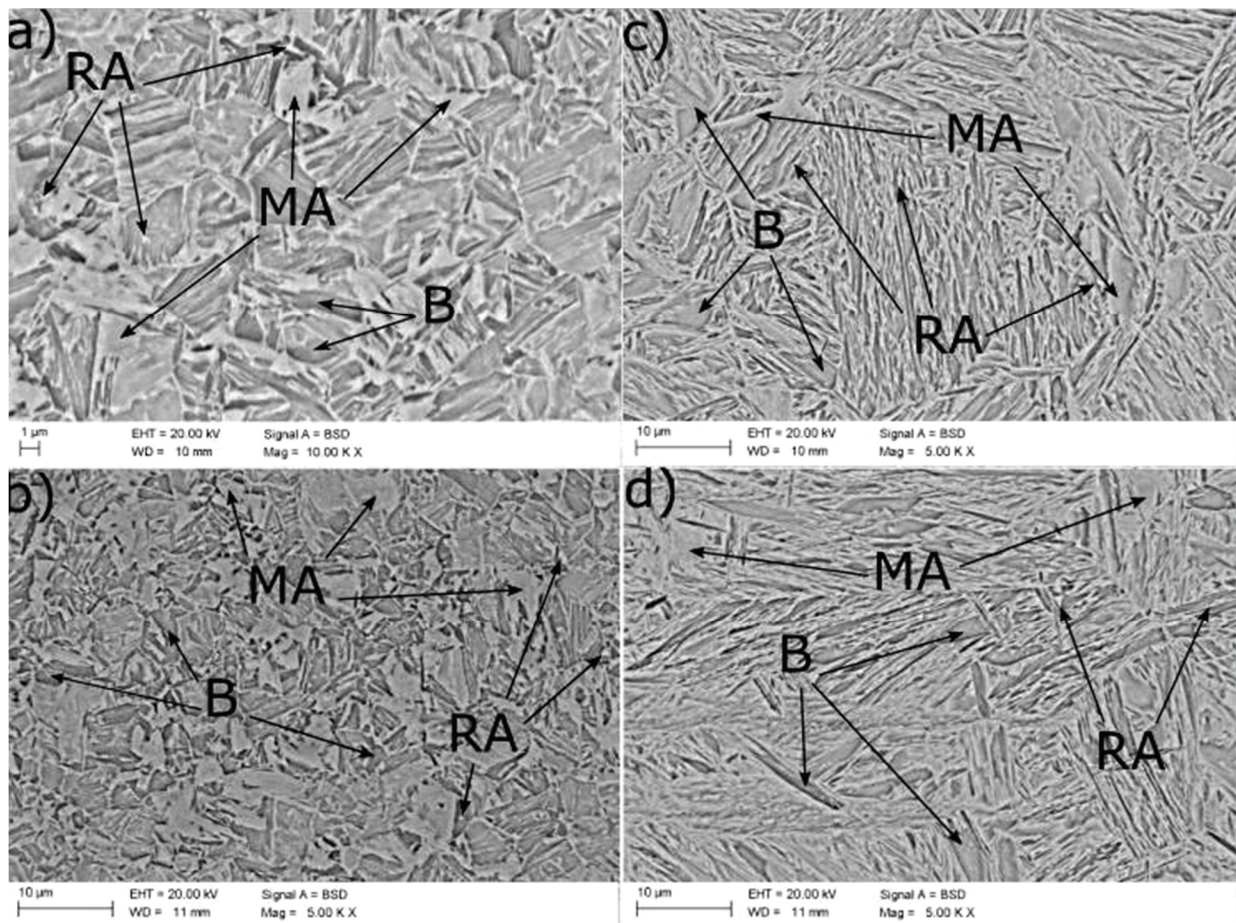


Figure 3 SEM microstructures of heat affected zone for different power distributions: (a, b) CP steel with 50:50 and 70:30 % power distribution, (c, d) TRIP steel with 50:50 and 70:30 % power distribution

Figure 4 presents the hardness values of fusion and heat affected zone for CP and TRIP steels, welded with 50:50 and 70:30 % power distribution. It can be seen that the hardness of CP steel is lower compared to the TRIP steel independently on a power distribution. In case of CP steel the hardness of fusion zone is lower compared to the heat affected zone. The maximum value of hardness in FZ is 363 HV1 in case of 50:50 % power distribution. The change of power distribution to 70:30 % leads to a decrease in hardness of this zone by 16 HV1. A similar tendency can be seen in HAZ, but the change of hardness is smaller. In case of TRIP steel the maximum hardness of FZ is 450 HV1 for 50:50 % power distribution and decreases to 418 HV1 for 70:30 %. The hardness of HAZ decreases with the increasing power of the first beam. The change of hardness is bigger in comparison to the HAZ of CP steel. The higher hardness value of TRIP steel is due to its higher carbon equivalent compared to the CP steel.

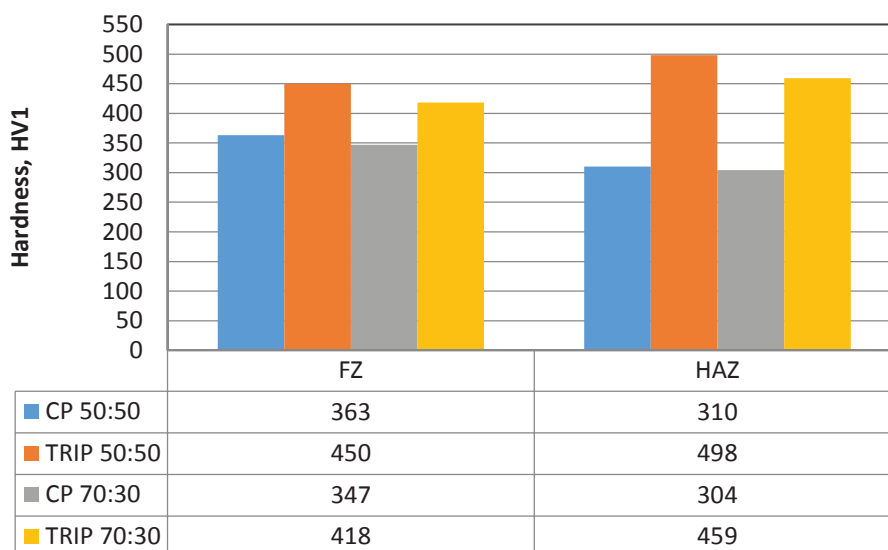


Figure 4 The hardness values of FZ and HAZ for CP and TRIP steels welded with 50:50 and 70:30 % power distribution

4. CONCLUSION

The use of twin-spot laser welding influences the microstructure and hardness of both steels. The presence of second beam increases the heat input into a material leading to a decrease in a cooling rate. The slower cooling stimulates tempering-like processes both in fusion and heat affected zones. The main difference in terms of the microstructure between complex phase and TRIP steels is the martensite morphology. The CP steel has more blocky morphology whereas the higher hardenability of TRIP steel results in its lath-like morphology. Tempering-like processes decrease the hardness of welds compared to single spot laser welding. The power distribution has an impact on properties of laser welds. In both cases the increase of the power of the first beam leads to a decrease in hardness of fusion and heat affected zones. In case of TRIP steel the change of hardness is much higher. Because of higher carbon equivalent of TRIP steel its hardness is higher compared to the CP steel. The highest hardness of HAZ (app. 500 HV1) shows the TRIP steel whereas the CP steel has a maximum hardness in its fusion zone. This different behaviour requires further investigations.

REFERENCES

- [1] JANICKI, D. Disc laser welding of armor steel. *Archives of Metallurgy and Materials*, 2014, vol. 59, pp. 1641-1646.
- [2] GORKA, J. Weldability of thermomechanically treated steels having a high yield point. *Archives of Metallurgy and Materials*, 2015, vol. 60, pp. 469-475.
- [3] KUC, D., HADASIK, E., NIEWIELSKI, G., SCHINDLER, I., MAZANCOVA, E., RUSZ, S., KAWULOK, P. Structural and mechanical properties of laboratory rolled steels high-alloyed with manganese and aluminium. *Archives of Civil and Mechanical Engineering*, 2012, vol. 12, p. 312-317.
- [4] MAZANCOVA, E., WYSLYCH, P., MAZANEC, K. Physical metallurgy of granular bainite. *Metallic Materials*, 1995, vol. 33, pp. 94-104.
- [5] WEGLOWSKI, M.S., STANO, S., MICHTA, G., OSUCH, W. Structural characterization of Nd: YAG laser welded joint of dual phase steel. *Archives of Metallurgy and Materials*, 2010, vol. 55, p. 211-220.
- [6] LISIECKI, A. Welding of thermomechanically rolled fine-grain steel by different types of lasers. *Archives of Metallurgy and Materials*, 2014, vol. 59, pp. 1625-1631.
- [7] DOBRZANSKI, L..A., GRAJCAR, A., BOREK, W. Microstructure evolution of C-Mn-Si-Al-Nb high-manganese steel during the thermomechanical processing. *Materials Science Forum*, 2010, vol. 638-642, pp. 3224-3229.

- [8] GRAJCAR, A., ROZANSKI, M., STANO, S., KOWALSKI, A. Microstructure characterization of laser-welded Nb-microalloyed silicon-aluminum TRIP steel. *Journal of Materials Engineering and Performance*, 2014, vol. 23, pp. 3400-3406.
- [9] JABLONSKA, M., SMIGLEWICZ, A. A study of mechanical properties of high manganese steels after different rolling conditions. *Metalurgija*, 2015, vol. 54, p. 619-622.
- [10] RADWANSKI, K., WROZYNA, A., KUZIĄK, R. Role of the advanced microstructures characterization in modeling of mechanical properties of AHSS steels. *Materials Science and Engineering A*, 2015, vol. 639, pp. 567-574.
- [11] LISIECKI, A., BURDZIK, R., SIWIEC, G., KONIECZNY, L., WARCZEK, J., FOLEGA, P., OLEKSIĄK, B. Disc laser welding of car body zinc coated steel sheets. *Archives of Metallurgy and Materials*, 2015, vol. 60, pp. 2913-2922.
- [12] OPIELA, M. Thermodynamic analysis of the precipitation of carbonitrides in microalloyed steels. *Materiali in Tehnologije*, 2015, vol. 49, pp. 395-401.
- [13] KUCEROVA, L., JIRKOVA, H., MASEK, B. The effect of alloying on mechanical properties of advanced high strength steels. *Archives of Metallurgy and Materials*, 2014, vol. 59, pp. 1189-1192.
- [14] SKOLEK, E., WASIAK, K., SWIATNICKI, W.A. Structure and properties of the carburised surface layer on 35CrSiMn5-5-4 steel after nanostructirization treatment. *Materiali in Tehnologije*, 2015, vol. 49, pp. 933-939.
- [15] SKUBISZ, P., ADRIAN, H., SIŃCZAK, J. Controlled cooling of drop forged microalloyed-steel automotive crankshaft. *Archives of Metallurgy and Materials*, 2011, vol. 56, pp. 93-107.